Near-Tropopause Vertical Motion within the Trailing Stratiform Region of a Midlatitude Squall Line

RICHARD H. JOHNSON, WILLIAM A. GALLUS, JR. AND MICHAEL D. VESCIO

Atmospheric Science Department, Colorado State University, Fort Collins, Colorado

(Manuscript received 15 December 1989, in final form 16 April 1990)

ABSTRACT

Rawinsonde observations have been used to determine the flow structure in the vicinity of the tropopause atop the trailing stratiform precipitation region of an intense midlatitude squall line. Computations of vertical motion using the kinematic and thermodynamic methods show (i) upward motion in the mid- to upper troposphere within the stratiform cloud and (ii) downward motion in a thin layer 2–3 km deep centered near the tropopause at cloud top. The latter feature, which has received little attention and explanation, has recently been reported to exist above stratiform rain areas in the tropics, as measured directly by a wind profiler on the tropical western Pacific island Pohnpei.

The thin layer of sinking at the top of the trailing stratiform region occurs along the sloping upper cloud boundary and is associated with downward-sloping isentropes in the lower stratosphere to the rear of the convective line. The deformation of the isentropes is associated with an upward bulging of the tropopause, presumably caused by strong ascent in the convective line and/or mesoscale ascent aloft in the squall line system. In computations involving the thermodynamic method, the diagnosed sinking is greatest when cloud-top radiative cooling is included, but it occurs even without it. Comparison of results from the various methods, however, suggests that radiative cooling at cloud top exists and is important, and it may have an amplitude on the order of 0.5°C h^{-1} as determined by Webster and Stephens. The strong cooling at the top of mesoscale convective systems such as these suggests a possible mechanism for dehydration of the lower tropical stratosphere that does not require a primary transport of water vapor from a particularly cold tropopause region such as the Indonesian maritime continent.

1. Introduction

A prominent feature of squall lines with trailing stratiform precipitation is a mesoscale region of ascending front-to-rear flow in the mid- to upper troposphere extending from near the 0°C level to the tropopause (Houze 1977; Zipser 1977). This ascent, at times reaching 0.5 to 1.0 m s^{-1}, is driven primarily by latent heat release within the stratiform cloud (Brown 1979). Recently, observational studies of the vertical motions in mesoscale convective systems were reviewed by Houze (1989). Generally, rawinsonde or Doppler radar data show this rising motion to fall off to near zero around the tropopause (Ogura and Liou 1980; Gamache and Houze 1982; Rutledge et al. 1988). However, in a recent study Balsley et al. (1988) have shown, using a vertically directed 50 MHz radar wind profiler at Pohnpei in the tropical western Pacific, a more complicated behavior to the vertical motion near the tropopause in light or stratiform rain situations. Specifically, they found (i) a secondary peak in upward motion in the troposphere near cloud top and (ii) just above this peak (extending into the lower stratosphere) a shallow layer of relatively strong, downward motion, having speeds locally up to 10 to 15 cm s^{-1}.

The findings of Balsley et al. (1988) are significant since they represent the first direct measurements of vertical motion (integration of the mass continuity equation is not required) at and above the tops of mesoscale stratiform cloud systems. Houze (1989) has pointed out that the lower-stratospheric descent detected by Balsley et al. remains to be explained but may be associated with strong divergent horizontal outflow that characteristically occurs at the tops of mesoscale convective systems (Ninomiya 1971; Maddox 1980; Fritsch and Maddox 1981; Maddox et al. 1981). This descent in the lower stratosphere is a feature that has previously gone largely unnoticed and, if it occurs generally, could have important implications regarding cloud-top radiative processes. However, the measurements taken on Pohnpei lack supporting information about cloud and precipitation structures since ground-based weather radar data were not available (only surface rainfall rates were recorded). Therefore, the relationship of the vertical motion to specific cloud features could not be determined. It is important to examine other datasets to see if similar vertical motion patterns occur elsewhere and, if so, to determine their relationship to the cloud and precipitation structures.

Corresponding author address: Richard H. Johnson, Dept. of Atmospheric Science, Colorado State University, Fort Collins, Colorado 80523.

The recent Oklahoma–Kansas Preliminary Regional Experiment for STORM-Central (OK PRE-STORM) has afforded, probably for the first time, an opportunity for a detailed investigation of this matter.

While most computations of vertical motion based on the kinematic method have not shown downward motion near the tropopause within the stratiform cloud portions of mesoscale convective systems, there have been several exceptions. In the study of Winter MONEX mesoscale anvil cloud systems, Johnson and Young (1983) discovered a region of sinking motion and an apparent heat sink (using the terminology of Yanai et al. 1973) near the top of the deep anvil clouds and suggested the heat sink may have been an indication of infrared radiative cooling off cloud tops. Kessinger et al. (1987) found within the trailing stratiform cloud region of an Oklahoma squall line a region of descent (up to 30 cm s^{-1}) centered near the tropopause and extending several km above and below it. Brandes (1990) also computed near-tropopause subsidence and detected lower stratospheric warming to the rear of a mesoscale convective system observed during the OK PRE-STORM. It is the purpose of this paper to present further observational evidence of sinking atop trailing stratiform clouds, which tends to support the Balsley et al. (1988) results, and to put these findings into the proper context of the overall circulation of squall line systems. Possible implications of the results for the troposphere–stratosphere exchange of water vapor will also be discussed.

2. Procedures

The kinematic method involves vertical integration of the mass continuity equation,

$$\overline{\nabla \cdot \mathbf{v}} + \frac{\partial \bar{\omega}}{\partial p} = 0 \qquad (1)$$

where overbar denotes an area average, $\nabla \cdot \mathbf{v}$ is the horizontal divergence, and $\omega = dp/dt$ is the vertical p-velocity. Normally, the divergence is adjusted to achieve mass balance in the column. This can be accomplished through upward integration of (1) from the surface, where $\bar{\omega}$ is set to zero (if the surface is flat), to some high level near the tropopause, where $\bar{\omega}$ is again set to zero. Errors in vertical motion encountered by this procedure are often greatest near the tropopause as a result of greater inherent errors in measurement at high levels and the accumulation of errors from below, so that computed values near the tropopause are normally viewed with caution. An approach that can partially reduce potential errors in the upper troposphere is the downward integration of (1) from the lower stratosphere. Such a procedure will be one of those used here.

One may also alternatively compute vertical motion from the first law of thermodynamics (Nitta 1977):

$$\bar{\omega} = \left[\frac{\partial \bar{\theta}}{\partial t} + \overline{\mathbf{v} \cdot \nabla \theta} - \frac{(p_o/p)^{\kappa}}{c_p} Q_R\right] \Big/ \left(-\frac{\partial \bar{\theta}}{\partial p}\right), \qquad (2)$$

where overbar denotes an area average, θ potential temperature, Q_R the radiative heating rate, c_p the specific heat at constant pressure, $\kappa = R/c_p$ and $p_o = 1000$ mb. In (2) we have neglected (i) latent heat exchanges since we will be using this expression only in the extremely cold tropopause regions (above 250 mb) and (ii) convergence of eddy heat fluxes, assumed to be small atop the stratiform cloud. A problem with (2) is that Q_R is unknown. The sensitivity of the computed $\bar{\omega}$ to Q_R will be examined.

In this study vertical motion will be computed using the following four procedures:

1) Upward integration of (1) using the procedure of O'Brien (1970) and setting $\bar{\omega} = 0$ at the surface and $p = 125$ mb (the tropopause in our case is near 150 mb);

2) Downward integration of (1) from 100 mb (assuming $\bar{\omega} = 0$ there) with no adjustments;

3) Solution of (2) above 250 mb assuming $Q_R = 0$; and

4) As in 3, except assuming $Q_R \neq 0$.

3. Data

Observations are taken for a squall line that passed through Kansas and Oklahoma during OK PRE-STORM on 10–11 June 1985. This squall line has been the subject of several investigations (Augustine and Zipser 1987; Rutledge and MacGorman 1988; Rutledge et al. 1988; Johnson and Hamilton 1988; Zhang et al. 1989; Zhang and Gao 1989). Sounding data taken at 90-min intervals from 0430 to 0730 UTC have been used by Johnson and Hamilton (1988) to form a composite of the flow field at 0600 UTC. The horizontal spacing of the composited data (~80 km), while insufficient to resolve motions in the leading convective line, is marginally sufficient to resolve the mesoscale circulations in the 200 km stratiform portion of the squall line. We will use these composited data to compute $\bar{\omega}$ (on a 50 km grid) from (1) and (2). In (2), $\partial \bar{\theta}/\partial t$ is computed with a centered time difference using noncomposited gridded fields of $\bar{\theta}$ at 0430 and 0730 UTC.

4. Results

a. Analyses at mature stage (0200 UTC)

When the squall line was in its most intense stage (around 0200 to 0300 UTC), its position relative to the sounding network was not optimum for determining vertical motion over the stratiform region. Nevertheless, some of the analyses that can be done at this time illustrate the same features that are observed in greater quantitative detail at 0600 UTC (the latter to be presented in the next subsection b.).

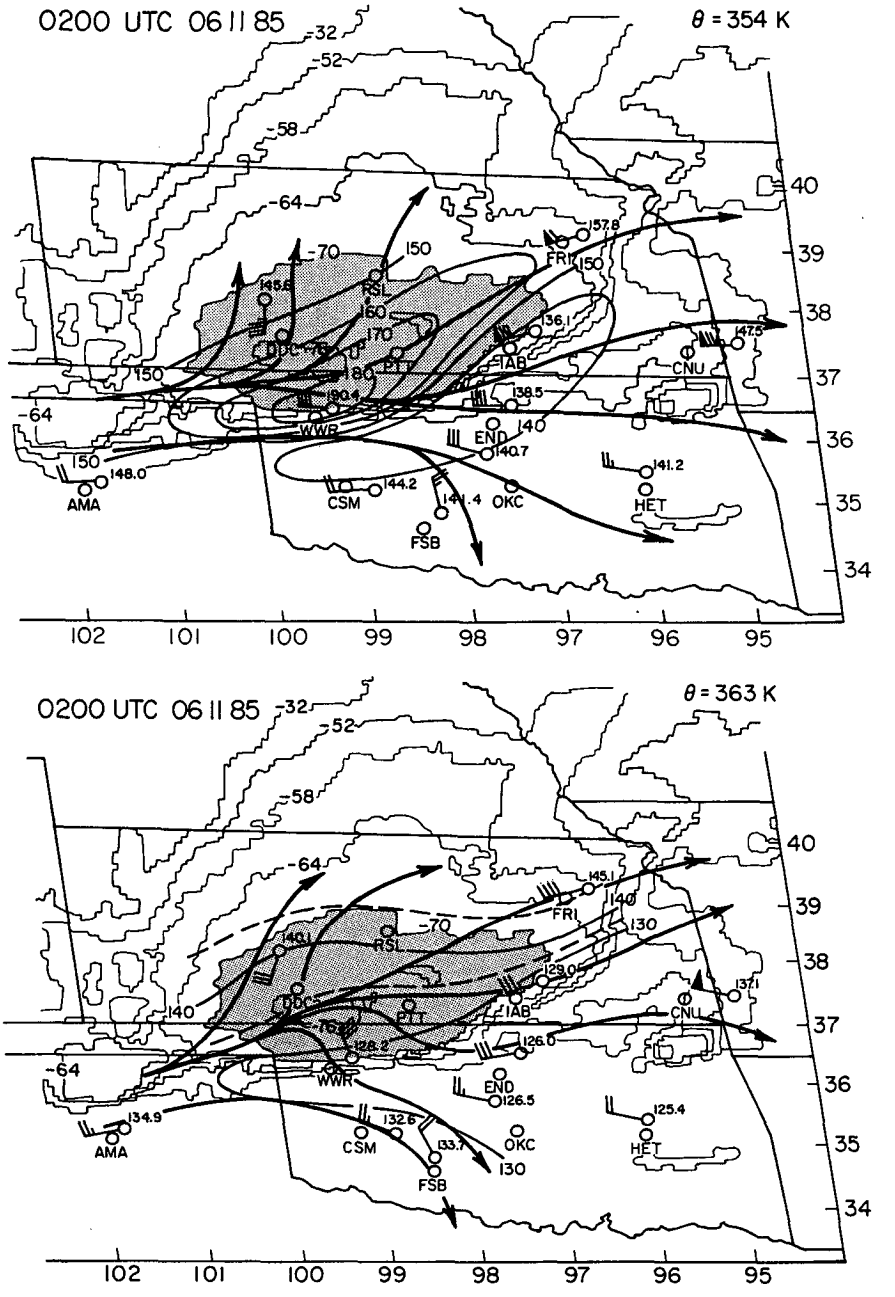

FIG. 1. Streamlines and pressure (mb) of the (a) 354 K and (b) 363 K isentropic surfaces over Kansas and Oklahoma at 0200 UTC 11 June 1985. Satellite IR brightness temperatures (°C) are also indicated, with values < −70°C shaded.

In Fig. 1a an analysis of pressure and streamlines on the 354 K isentropic surface at 0200 is shown. Also shown is the field of IR brightness temperature. Radar data (Rutledge et al. 1988; Johnson and Hamilton 1988) indicate that at this time the squall line was characterized by a narrow (~40 km) leading convective line along the zone of sharp temperature gradient on the southern periphery of the cloud mass and a trailing stratiform region (~100 to 200 km wide) to the north. The lowest cloud-top temperatures (< −76°C) were positioned behind the leading convective line. Within ~100 km of the leading convective line this isentropic surface resided primarily in the upper troposphere. This θ surface protruded downward along the axis of the leading convective line as a result of latent heat release in deep convection there (the exceptionally warm data point near WWR is from the 0130 UTC sounding at Woodward OK). The flow was

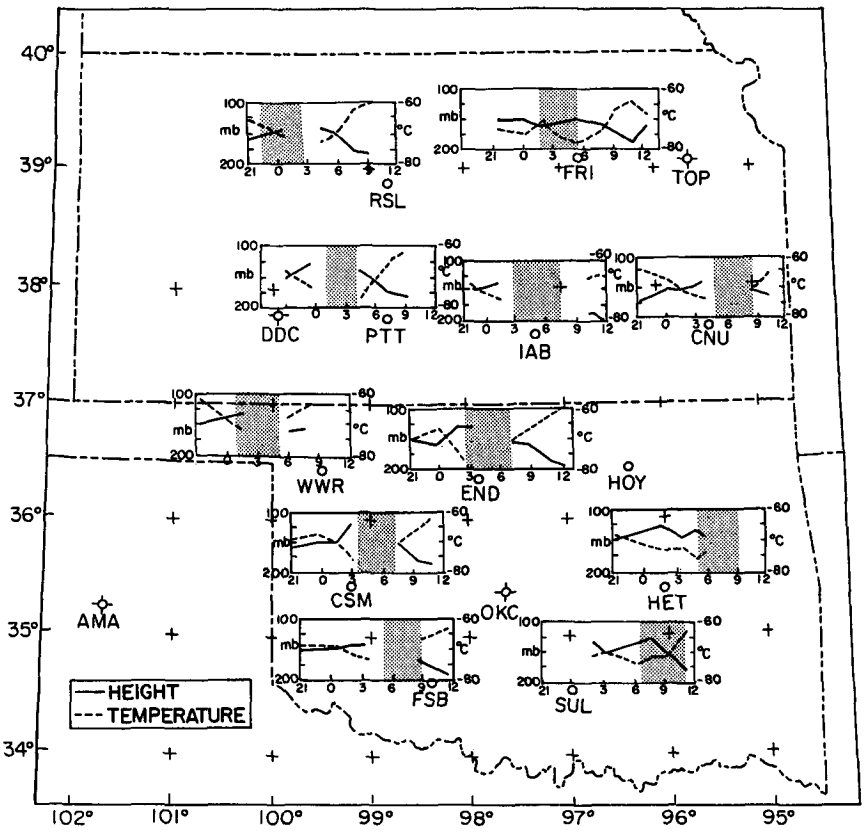

FIG. 2. Time series of tropopause pressure (mb, solid) and tropopause temperature (°C, dashed) at supplemental sounding sites from 2100 UTC 10 June to 1200 UTC 11 June 1985. Shaded region indicates period of squall line passage.

generally diffluent along this axis so that one can infer, assuming adiabatic motions, (i) rising motion several hundred kilometers to the rear of the convective line within the trailing stratiform region and (ii) rising motion in a very narrow zone along the leading edge of the upper-level cloud canopy. The motions, of course, were not strictly adiabatic; however, at these very high levels latent heating in the stratiform region was very small. Radiative cooling may not be negligible atop the stratiform region, but it is not strong enough to change the inference from Fig. 1a of rising motion at these levels within the stratiform cloud (as will be confirmed later)[1]. Using storm-relative wind speeds and assuming adiabatic flow, upward motion of 30 cm s^{-1} is computed between 150 and 160 mb in the stratiform region between DDC and RSL in Fig. 1a at 0200 UTC.

The slightly higher flow on the 363 K isentropic surface (at the tropopause and in the lower stratosphere) is depicted in Fig. 1b. Although the flow is still diffluent at this level, the pressure gradient on this isentropic surface over the stratiform region has reversed, yielding an inferred downward motion at this higher level. Again assuming adiabatic motion, we compute a subsidence of 5 cm s^{-1} between 135 and 140 mb in the DDC to RSL area. Later computations will show that the diagnosed subsidence is even greater if radiative cooling at cloud top is included.

Isentropic analyses have also been completed at 0300 UTC (but not shown) with results very similar to those in Fig. 1 being obtained.

b. Analyses during dissipating stage (0600 UTC)

At 0600 UTC there were sufficient data within the trailing cirrus and stratiform canopy to permit reasonably reliable computations of vertical motion. However, despite the improvement in data coverage at this time, a significant gap in rawinsonde data existed within the precipitating stratiform region as balloons had difficulty, in many instances, in ascending above the 0°C level within these cloud systems.

In Fig. 2 time series of tropopause heights before, during, and after the squall line passage are shown at each of the PRE-STORM sounding sites. The fre-

[1] Radiative heating (as opposed to cooling) at cloud top is not expected to occur since (i) the upper-level cloud developed around and after sunset and (ii) most of the stratiform cloud layer was optically thick, so that IR heating from below was not important (Webster and Stephens 1980).

quently missing data during squall passage (hatched area) are evident. A general pattern of rising tropopause prior to the squall line arrival and descending tropopause following passage can be seen. Typical changes in the tropopause height were −25 mb (+1 km) before and +50 mb (−2 km) after passage. The descent after passage may be partially attributed to the advance of an upper-level trough into the region. A corresponding tropopause-level cooling up to 10 K was also observed at many stations during the squall line passage (Fig. 2). Similar modulations of the tropopause height and cooling at the tropopause level were detected during the passage of squall lines over the South China Sea to the north of Borneo during Winter MONEX (Johnson and Kriete 1982) and also within other midlatitude mesoscale convective systems (Fritsch and Maddox 1981; Ninomiya et al. 1981; Heymsfield and Blackmer 1988).

Before showing computations of vertical motion across the entire squall line using (2), we first focus on a smaller domain within which there is a good coverage of sounding data extending through the entire troposphere. Specifically, vertical motion has been computed using the four procedures outlined in section 2 for the quasi-rectangular domain in Fig. 3, which is positioned toward the rear of the upper-level stratiform cloud outside the area of surface rainfall. The cloud-top temperatures at this time increased somewhat since 0200 (Fig. 1) and there is a more broken appearance to the upper cloud surface.

The vertical motion computed by the four procedures (averaged over the polygon area in Fig. 3) is shown in Fig. 4. The analysis region is in the far rear portion of the stratiform cloud where the cloud-layer depth is only 2–4 km. Cloud base is approximated by the level where the relative humidity (with respect to ice) equals 80%. Satellite IR data indicate the top of

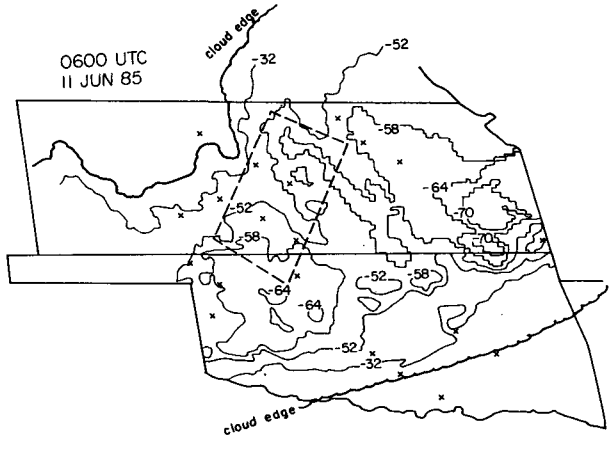

FIG. 3. Satellite IR brightness temperatures at 0600 UTC 11 June 1985. Vertical motion computational domain is indicated by dashed lines. *X* denotes stations with sounding data extending to tropopause level during 0430–0730 UTC composite period.

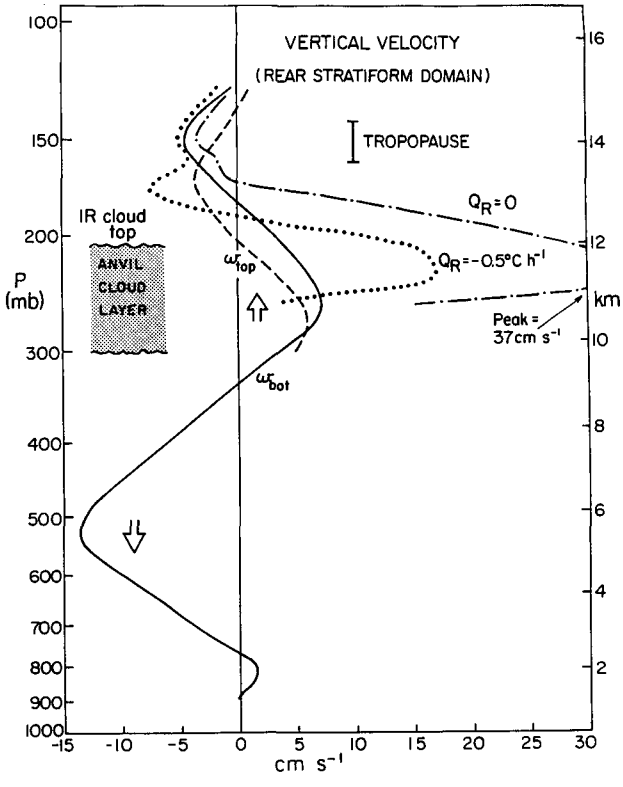

FIG. 4. Vertical velocity (cm s^{-1}) for the rear stratiform domain shown in Fig. 3 as determined by the four procedures described in section 2. Average cloud layer depth and tropopause height within domain are illustrated. w_{bot} indicates bottom-up integration and w_{top} top-down integration.

the cloud layer to be near 12 km or 200 mb; however, it probably extends ~1 to 2 km higher to near the tropopause level in the form of thin stratiform cloud—i.e., containing small concentrations of ice particles [as found by high-flying ER-2 aircraft within EMEX/STEP (Equatorial Mesoscale Experiment/Stratosphere Troposphere Exchange Project 1987) mesoscale anvil clouds; G. L. Stephens and H. Selkirk 1989, personal communication]. Remarkably, all four methods yield sinking motion over a ~2–3 km layer centered near the tropopause. The peak subsidence in this layer for the two kinematic methods is 3–5 cm s^{-1}. The top-down integration gives a peak approximately 1 km lower than that for the bottom-up integration. Both kinematic methods yield upward motion up to 6–7 cm s^{-1} within the anvil cloud layer between 9 and 12 km. Below the cloud layer sinking motion is diagnosed, extending down to 750 mb. This sinking occurs within a rear inflow jet that descends along the back edge of the stratiform region (Johnson and Hamilton 1988). In the lowest 2 km there is weak upward motion. This feature is likely associated with the weak cloud line observed to the rear of the squall line.

The computation of $\bar{\omega}$ assuming $Q_R = 0$ (Fig. 4) gives subsidence up to 3 cm s^{-1} between 13 and 15

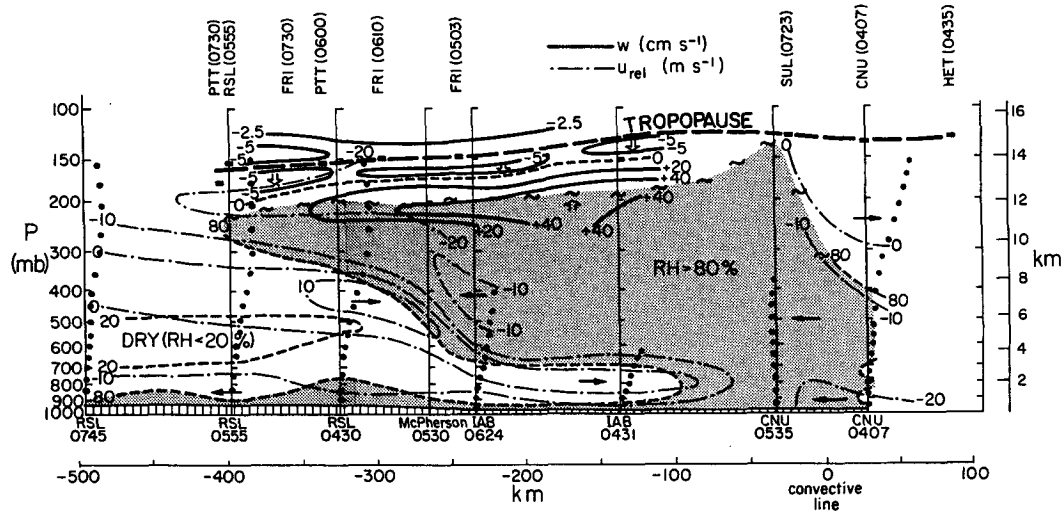

FIG. 5. Vertical cross section showing system-relative flow (m s^{-1}; dash–dot lines) along direction of squall line motion, vertical motion (cm s^{-1}; heavy solid lines) at stratiform cloud top averaged along entire line in Kansas and Oklahoma; and relative humidity (with respect to ice at temperatures below freezing; thin dashed lines; shaded area is for relative humidity > 80%) based on data composited about 0600 UTC 11 June 1985. Squall line speed and direction of motion are 15 m s^{-1} and toward 130°, respectively. Dots indicate balloon positions and short heavy bars the tropopause height at selected sounding sites (denoted at top).

km and a sharp peak of rising motion below, reaching 37 cm s^{-1} at 11.5 km or 225 mb. The amplitude of the sinking at 0600 UTC is in reasonable agreement with that deduced earlier at 0200 UTC (section 4a). Radiative cooling is included in (2) by assuming $Q_R = -0.5$°C h^{-1}, based on the work of Webster and Stephens (1980). In this computation a constant value is assumed at all levels for simplicity, although it is recognized that this assumption is deficient.[2] For optically thin upper-level cloud layers, a net radiative warming within the layer can occur (Ackerman et al. 1988); however, our cloud system is optically thick over most of the area of interest. The inclusion of radiative cooling has the effect of amplifying and lowering the subsidence peak near the tropopause and reducing the amplitude of the upward motion peak below, bringing it more in line with the kinematically-determined values.

A broader perspective of the squall line is shown in Fig. 5. This cross section is oriented NW–SE (310°–130°) across the Kansas portion of the line (except for the one data point for the tropopause height at Sulphur, OK, which is derived from the only sounding within 1.5 h of 0600 UTC that was able to penetrate the convective-to-stratiform precipitating portion of the storm). This cross section is similar to that in Fig. 16 of Johnson and Hamilton (1988), but it has been extended southeastward to include the leading portion of the line. The main features of the system-relative flow below cloud top were discussed in that paper, namely (i) a front-to-rear flow from low levels ahead of the line sloping upward to high levels in the rear, (ii) a rear inflow jet extending from the upper troposphere behind the storm to near the surface behind the leading convective line and (iii) a low-level front-to-rear outflow at the surface.

Vertical motion computed from (2) and averaged in the along-line direction across the entire stratiform region is illustrated above 250 mb in Fig. 5. Here we have set $Q_R = -0.5$°C h^{-1} down to 2 km below the tropopause level and $Q_R = 0$ below. Consistent with Fig. 4, a thin layer of subsidence exceeding 5 cm s^{-1} is diagnosed from just above to 1 km below the tropopause, sloping downward toward the rear of the storm over the trailing stratiform region. Three features—tropopause height, axis of maximum downward motion, and IR-inferred cloud top—all show this consistent downward slope toward the rear of the line. The axis of maximum sinking lies just below the tropopause. This pattern of subsidence is also consistent with that deduced on a somewhat smaller scale near the tropopause downstream of severe-storm overshooting cloud tops (Heymsfield et al. 1983; Adler and Mack 1986; Heymsfield and Blackmer 1988). The relationship of these latter findings, however, to mesoscale convective systems needs further study.

If, on the other hand, we assume $Q_R = 0$ everywhere, sinking is still deduced, but its maximum amplitude is reduced to 2–3 cm s^{-1} and the axis of the peak is shifted upward to near the tropopause level (as depicted in Fig. 4). On the basis of the work of Webster and Ste-

[2] The neglected latent heat release term in (2) reaches one-tenth the magnitude of Q_R at 250 mb, so values are not shown below this level.

phens (1980) and others, and the occurrence of this cloud system at night (so that short wave absorption is absent), it appears that the results for $Q_R \neq 0$ in Fig. 5 provide a slightly more realistic depiction of the vertical motion field than those obtained for $Q_R = 0$.

In a portion of the region (−100 to −300 km in Fig. 5) behind the leading convective line, downward motion along cloud top was not obtained using the kinematic method at 0600 UTC. The inability to obtain agreement between the thermodynamic and kinematic methods in this region is due to the lack of soundings reaching higher levels there (Fig. 3). The thermodynamic method is probably less sensitive to data inadequacies in this region because it requires only data from the levels of interest. To the extent that interpolations across this region have errors, there will be errors in the analysis; however, the deduced flow is qualitatively the same as that inferred from the isentropic analyses in Fig. 1. Furthermore, and more importantly, we repeated an analysis like that in Fig. 5 using a 3-h composite at 0730 UTC, incorporating 0900 UTC data that had considerably better coverage over the stratiform precipitation region. Here again we obtained sinking motion all along the top of the stratiform region using both the kinematic and thermodynamic methods.

c. *Comparison with tropical results*

In Fig. 6 vertical motion over the stratiform domain shown in Fig. 3 is compared to that obtained by Balsley et al. (1988) from a wind profiler at Pohnpei (7°N, 157°E). Vertical velocity is plotted as a function of height normalized by the tropopause height in order to scale the data relative to cloud top. The tropopause height in the tropical case is 2.5 km higher than the midlatitude case. Values of computed w are the same as those shown in Fig. 4, except that the bottom-up integration results below $\hat{z} = 0.75$ are for the *entire* stratiform region (to enable a more appropriate comparison with the Balsley et al. general stratiform results).

It can be noted from Fig. 6 that the kinematic method yields results in qualitative agreement with the wind profiler results. Namely there is downward motion within a thin layer near the tropopause, rising motion in the troposphere peaking near $\hat{z} = 0.6$, and w approaching zero near $\hat{z} = 0.25$ to 0.3. The top-down w profile shows maximum sinking near $\hat{z} = 0.93$–0.95 (approximately 1 km below the tropopause). Since the top–down integration is expected to be more accurate than the bottom–up near cloud top, this finding tends to support the Balsley et al. (1988) results. The amplitude of the sinking motion in the tropical study is greater than that determined here. It is probable, however, that the relatively coarse horizontal resolution of the data in our case contributes to a reduction in diagnosed amplitude of vertical motion from its true value locally over the stratiform region.

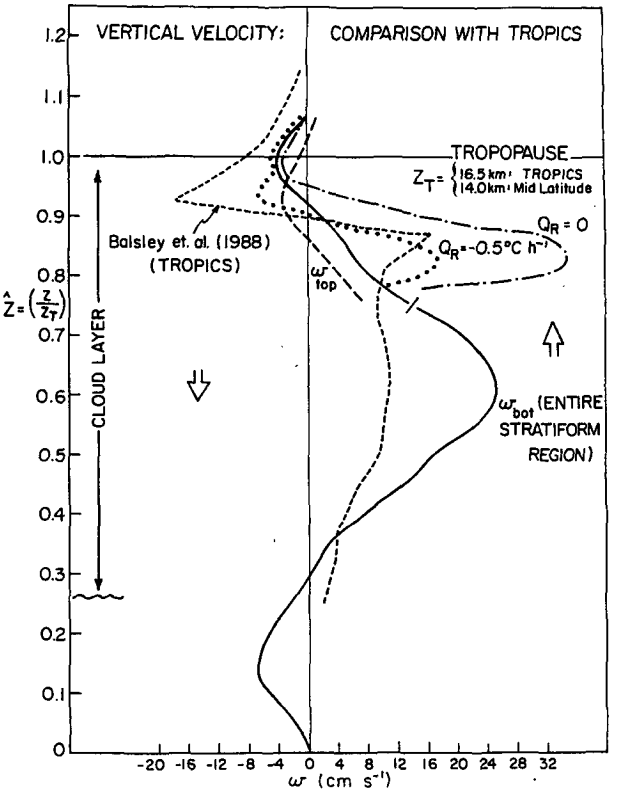

FIG. 6. Vertical velocity (cm s^{-1}) as a function of height normalized to the tropopause elevation for four computational procedures described in section 2 and from Balsley et al. (1988). The w_{bot} profile below $\hat{z} = 0.75$ is for the entire stratiform region to better correspond to the Balsley et al. entire stratiform rain area results. Above this level, the four curves computed from this study are for domain in Fig. 3, but from Fig. 5 are expected to be similar to those along the entire stratiform region.

Absent from the kinematically-determined profiles, however, is a layer of enhanced upward motion between $\hat{z} = 0.8$ and 0.9 as found by Balsley et al.[3] This latter layer, however, in addition to the upper layer of sinking, is observed in the w profiles determined from the thermodynamic budget (Fig. 6). The best agreement between the wind profiler-derived structure and that determined from (2) is for the $Q_R = -0.5$°C h^{-1} case. In particular, the normalized levels of upward and downward motion maxima are in reasonably good agreement. Nevertheless, a sharp transition between upward and downward motion near the tropopause is also evident for $Q_R = 0$, suggesting that this feature is not exclusively a result of cloud-top radiative cooling. The near-tropopause downward motion occurs even if radiative cooling is neglected.

[3] Considering the differences between the methodologies and analysis regions of our study and that of Balsley et al. (1988), we regard conclusions drawn from comparisons of this secondary feature to be tentative, at best.

The secondary upward motion peak between $\hat{z} = 0.8$ and 0.9 in Balsley et al. (1988), while conceivably being supported by the results from (2), is not necessarily confirmed. The procedures involving (2) could not be reliably extended to lower levels to determine whether a secondary peak exists since terms involving condensation and freezing are not known. Also, the kinematic methods do not yield a secondary peak in vertical motion. Interestingly, however, a secondary upper-level peak (near 12 km) in the stratiform region was obtained from Doppler radar EVAD analyses by Rutledge et al. (1988) around 0340 UTC. On the other hand, these EVAD analyses do not indicate downward motion near the tropopause. In the EVAD procedure, however, ω is not determined directly, but rather from (1) by setting $\omega = 0$ at the radar-determined cloud top. Moreover, the determination of a thin layer of convergence at cloud top (necessary to obtain downward motion), where reflectivities are very weak, is unlikely within the capabilities of the EVAD procedure.

5. Discussion

a. Characteristics of near-tropopause descent

It was noted in section 4 that downward motion near the top of the stratiform cloud layer is evident without invoking radiative cooling (Figs. 4 and 6). Therefore, it can be argued that the presence of this sinking, while modulated by radiative effects, is independent of them and is associated with downward-sloping isentropes to the rear of the convective line. Specifically, there appears to be a deformation of the tropopause and quasi-isentropic flow along the line following its upward bulging during the passage of the leading convective line (Figs. 2 and 5). The upward bulging is presumed to be caused by strong ascent in the deep convective towers and/or mesoscale ascent aloft in the squall line system, both of which can produce cooling extending into the lower stratosphere (Fritsch and Brown 1982; Schlesinger 1984; Adler and Mack 1986; Heymsfield and Blackmer 1988). The detailed mechanism of tropopause lifting is not well known, however. In the 10–11 June case, uncertainty in its cause is highlighted by the fact that during the mature stage of the squall line, the satellite IR temperature minimum was 50 to 100 km behind the leading convective line (Zipser 1988). Similar cooling and elevated tropopauses have been observed above the eyes of hurricanes (Arakawa 1951; Koteswaram 1967; Gentry 1967). The deformation of θ surfaces by this process is shown in Fig. 7. The system-relative streamlines depict air descending along and slightly across these deformed θ surfaces in a thin layer from front to rear along the top of the stratiform cloud over a distance of several hundred km. If the flow were adiabatic, there would still be descent. It is the large horizontal dimension of this phenomenon that presumably allowed Balsley et al. (1988) to capture its structure readily from wind profiler time series.

The streamlines and θ-field in Fig. 7 provide a convenient depiction of diabatic processes within the entire squall line. If we treat the streamlines qualitatively as trajectories, then we can visualize diabatic heating ($d\theta/dt$, or the change in θ along trajectories) in several distinct regions: 1) strong (latent) heating at upper levels in the leading convective line, 2) moderate (latent) heating in the upper-level trailing stratiform region, 3) moderate (evaporative) cooling in the descending rear inflow jet and 4) moderate (radiative) cooling near cloud top. We cannot deduce the actual magnitude of cloud-top radiative cooling from our analysis; however, since the results including radiative cooling do provide better agreement with those of Balsley et al. (1988), it does appear that cloud-top cooling is an important process affecting the circulation atop stratiform cloud systems.

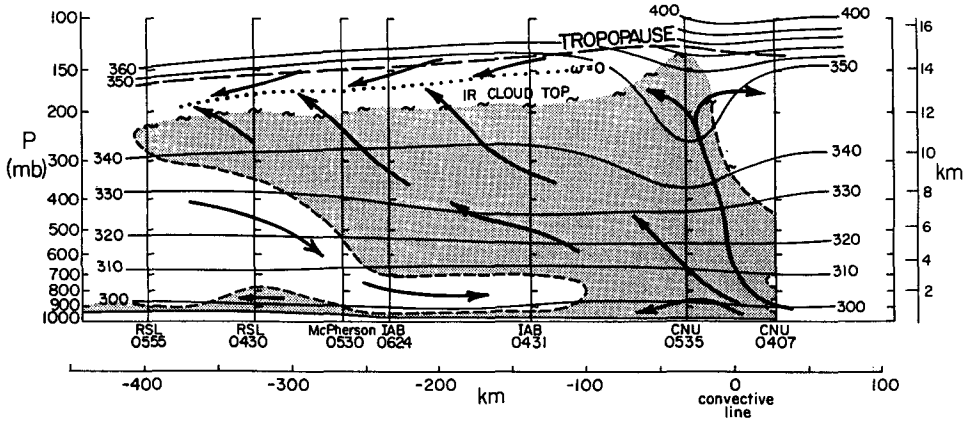

FIG. 7. Streamlines for system-relative flow and isentropes (K) along squall line direction of motion at 0600 UTC 11 June 1985. Relative humidity (with respect to ice at temperatures below freezing) greater than 80% is shaded. Streamlines along cloud top are based on an assumption of cloud-top radiative cooling of $-0.5°C\ h^{-1}$.

Another conclusion that may be drawn from these findings relates to the satellite depictions of the massive upper-level cloud system associated with this squall line and other mesoscale convective systems or mesoscale convective complexes (MCCs, Maddox 1980). Evident from Figs. 1 and 3 is a gradual increase in brightness temperature from a minimum just behind the leading edge to higher values at the rear. A similar character to the IR-inferred temperature pattern has been observed and discussed for cumulonimbus anvils near Panama (Danielsen 1982a; Ackerman et al. 1988). Ackerman et al. (1988) attribute the outward increasing brightness temperatures from a central cold core in their case to a corresponding outward decreasing optical depth. Danielsen (1982a) has noted from measurements of the thunderstorm anvils near Panama that the emissivity of these clouds reaches unity for depths exceeding approximately 2 km. Since over much of the area of interest the stratiform cloud depth in our case exceeds 5 km, it is then clear that the gradation in brightness over much of the upper-level canopy seen in Figs. 1 and 3 cannot be associated with emission from below the cloud layer. Assuming that the ice water content has a similar vertical distribution all along the top of the stratiform cloud region, this satellite depiction may itself illustrate the downward slope of the upper-level anvil cloud. Further, assuming front-to-rear system-relative flow, the satellite data may then be used qualitatively to infer gradual descent along cloud top.

b. Possible implications for troposphere–stratosphere exchange of water vapor

It has been argued by Brewer (1949) that the very low water vapor mixing ratios (<2–3 ppmv or parts per million by volume) in the lower stratosphere may be accounted for by ascent of tropospheric air through the extremely cold tropical tropopause, so that the air is effectively "freeze-dried." Measurements, however, from high-altitude aircraft over Brazil (Kley et al. 1979) and Panama (Danielsen 1982b; Kley et al. 1982) have shown that the water vapor mixing ratios just above the tropical tropopause are well below the saturation mixing ratio at the local tropopause temperature. These observations led Kley et al. (1979), Newell and Gould-Stewart (1981), and others to propose that the extremely dry lower-stratospheric air may be explained by horizontal transport from a colder region. Newell and Gould-Stewart (1981) suggested that the Indonesian maritime continent may be the focal region for the transport since it possesses the lowest tropopause temperatures in the world.

The results of this study, however, indicate that perhaps distant transport is not needed. The significant cooling aloft in the region of the leading convective line (up to 10 K) of this squall system and similar cooling found above other mesoscale convective systems in midlatitudes (Fritsch and Maddox 1981) and the tropics (Johnson and Kriete 1982) could provide for considerably enhanced freeze-drying in overshooting convective towers. For example, a reduction of the tropopause temperature by 5 K in the Panama region (using data from Danielsen 1982b) could, assuming irreversible ascent and fallout of ice, lead to dehydration locally to 3 ppmv—and a reduction by 8 K to 2 ppmv. Since organized mesoscale convective systems are prevalent throughout the tropics, dehydration could be operating within these systems on a global basis. Of course, this mechanism does not rule out the possibility of other mechanisms acting to dehydrate the lower stratosphere, such as distant transport or the incorporation of air from thin cirrus cloud layers into the lower stratosphere through net radiative heating (Lilly 1988; Ackerman et al. 1988).

6. Summary and conclusions

The kinematic and thermodynamic methods have been used to compute vertical motion in the vicinity of the tropopause above the trailing stratiform region of a squall line that occurred on 10–11 June 1985 during OK PRE-STORM. The objective has been to determine the detailed characteristics of the flow in a portion of squall line systems that has previously been poorly sampled, namely the region near stratiform cloud top. An additional objective has been to determine whether the recent wind-profiler results of Balsley et al. (1988) can be confirmed with high resolution rawinsonde data. Specifically, Balsley et al. have found a complicated behavior of the vertical motion near the tropopause in stratiform rain regions. They find a primary peak in upward motion in the middle of the stratiform cloud layer; a secondary peak near cloud top; and a relatively strong, shallow layer of downward motion extending from cloud top into the lower stratosphere. The findings of Balsley et al. are unique in that they represent the first direct measurements of vertical motion at and above the tops of mesoscale stratiform cloud systems. The thin layer of lower-stratospheric descent has not received much attention and, if it occurs generally, could have important implications regarding cloud-top radiative processes.

The results of our study confirm the findings of Balsley et al. (1988) concerning a thin layer of descent above stratiform cloud systems. Four separate computations indicate sinking motion up to 5 cm s^{-1} in a thin layer 2–3 km deep centered near the tropopause atop the stratiform cloud. Descent is diagnosed even if effects of radiative heating are neglected. Therefore, it is argued that the sinking, while modulated by radiative effects, is independent of them and is associated with downward-sloping isentropes to the rear of the leading convective line. Specifically, there appears to be a deformation of the tropopause and quasi-isentropic flow along it following its upward bulging during the passage of the convective line. Similar flow behavior

has been determined on a smaller scale downstream of severe-storm overshooting cloud tops (Heymsfield et al. 1983, Schlesinger 1984; Adler and Mack 1986; Heymsfield and Blackmer 1988). A schematic (Fig. 7) is presented to illustrate the system-relative front-to-rear descent along the top of the stratiform cloud region. Results from the thermodynamic method that include effects of cloud-top radiative cooling (obtained from Webster and Stephens 1980, as appropriate for our nighttime case) are in better agreement with both the Balsley et al. results and the kinematic method results, suggesting that radiative cooling exists and is important at the stratiform cloud top.

The pronounced upper-tropospheric and lower-stratospheric cooling associated with the squall line passage may play some role in the dehydration of the lower stratosphere. It has been observed in many areas of the tropics that the water vapor mixing ratio in the lower stratosphere is below the saturation mixing ratio at the local tropopause temperature. This observation has led some (e.g., Newell and Gould-Stewart 1981) to propose that the extremely dry lower-stratospheric air may be explained by horizontal transport from a colder region, such as the Indonesian maritime continent. The local cooling atop mesoscale convective systems, which are prevalent throughout the tropics, could remove this requirement for distant transport by providing for an enhanced freeze-drying of the air penetrating the lower stratosphere in overshooting convective towers and, assuming irreversible ascent and fallout of ice, dehydration to observed levels.

While the results for this case show strong evidence for cloud-top descent, there is clearly a need for additional measurements of this phenomenon. A particular problem with rawinsonde measurements in mesoscale convective systems is their frequent inability to ascend through the stratiform cloud region. Wind profilers can solve this problem and, when used in conjunction with Doppler radars, a more detailed mapping of the flow relative to the cloud system can be obtained. There is also a need to better relate these flow features to satellite measurements, particularly of cloud top temperature structure and precipitation characteristics of the convective systems (Ackerman et al. 1988; Simpson et al. 1988).

Acknowledgments. This research has been supported by the National Science Foundation, Atmospheric Science Division, under Grant ATM-8711649. The helpful comments of Professors Ed Zipser, Robert Houze, Mike Fritsch and Dr. Ben Balsley have been appreciated. We also thank Dr. Gerald Heymsfield for bringing to our attention related studies involving severe local storms.

REFERENCES

Ackerman, T. P., K.-N. Liou, F. P. J. Valero and L. Pfister, 1988: Heating rates in tropical anvils. *J. Atmos. Sci.*, **45**, 1606–1623.

Adler, R. F., and R. A. Mack, 1986: Thunderstorm cloud top dynamics as inferred from satellite observations and a cloud top parcel model. *J. Atmos. Sci.*, **43**, 1945–1960.

Arakawa, H., 1951: Analysis of the tropopause and stratospheric field of temperature of a mature typhoon. *Pap. Meteor. Geophys.*, **2**, 1–5.

Augustine, J. A., and E. J. Zipser, 1987: The use of wind profilers in a mesoscale experiment. *Bull. Amer. Meteor. Soc.*, **68**, 4–17.

Balsley, B. B., W. L. Ecklund, D. A. Carter, A. C. Riddle, and K. S. Gage, 1988: Average vertical motions in the tropical atmosphere observed by a radar wind profiler on Pohnpei (7°N latitude, 157°E longitude). *J. Atmos. Sci.*, **45**, 396–405.

Brandes, E. A., 1990: Evolution and Structure of the 6–7 May 1985 mesoscale convective system and associated vortex. *Mon. Wea. Rev.*, **118**, 109–127.

Brown, J. M., 1979: Mesoscale unsaturated downdrafts driven by rainfall evaporation: A numerical study. *J. Atmos. Sci.*, **36**, 313–338.

Danielsen, E. F., 1982a: Statistics of cloud cumulonimbus anvils based on enhanced infrared photographs. *Geophys. Res. Lett.*, **9**, 601–604.

——, 1982b: A dehydration mechanism for the stratosphere. *Geophys. Res. Lett*, **9**, 605–608.

Fritsch, J. M., and R. A. Maddox, 1981: Convectively driven mesoscale weather systems aloft. Part I: Observations. *J. Appl. Meteor.*, **20**, 9–19.

——, and J. M. Brown, 1982: On the generation of convectively driven mesohighs aloft. *Mon. Wea. Rev.*, **110**, 1554–1563.

Gamache, J. F., and R. A. Houze Jr., 1982: Mesoscale air motions associated with a tropical squall line. *Mon. Wea. Rev.*, **110**, 118–135.

Gentry, R. C., 1967: Structure of the upper troposphere and lower stratosphere in the vicinity of Hurricane Isabell, 1964. *Pap. Meteor. Geophys.*, **18**, 293–310.

Heymsfield, G. M., R. H. Blackmer Jr. and S. Schotz, 1983: Upper-level structure of Oklahoma tornadic storms on 2 May 1979. I: Radar and satellite observations. *J. Atmos. Sci.*, **22**, 1740–1755.

——, and ——, 1988: Satellite-observed characteristics of Midwest severe thunderstorm anvils. *Mon. Wea. Rev.*, **116**, 2200–2224.

Houze, R. A. Jr., 1977: Structure and dynamics of a tropical squall-line system observed during GATE. *Mon. Wea. Rev.*, **105**, 1540–1567.

——, 1989: Observed structure of mesoscale convective systems and implications for large-scale heating. *Quart. J. Roy. Meteor. Soc.*, **115**, 425–461.

Johnson, R. H., and D. C. Kriete, 1982: Thermodynamic and circulation characteristics of winter monsoon tropical mesoscale convection. *Mon. Wea. Rev.*, **110**, 1898–1911.

——, and G. S. Young, 1983: Heat and moisture budgets of tropical mesoscale anvil clouds. *J. Atmos. Sci.*, **40**, 2138–2147.

——, and P. J. Hamilton, 1988: The relationship of surface pressure features to the precipitation and air flow structure of an intense midlatitude squall line. *Mon. Wea. Rev.*, **116**, 1444–1472.

Kessinger, C. J., P. S. Ray and C. E. Hane, 1987: The Oklahoma squall line of 19 May 1977. Part I: A multiple Doppler analysis of convective and stratiform structure. *J. Atmos. Sci.*, **44**, 2840–2864.

Koteswaram, P., 1967: On the structure of hurricanes in the upper troposphere and lower stratosphere. *Mon. Wea. Rev.*, **95**, 541–564.

Lilly, D. K., 1988: Cirrus outflow dynamics. *J. Atmos. Sci.*, **45**, 1594–1623.

Maddox, R. A., 1980: Mesoscale convective complexes. *Bull Amer. Meteor. Soc.*, **61**, 1374–1387.

——, D. J. Perkey and J. M. Fritsch, 1981: Evolution of upper tropospheric features during the development of a mesoscale convective complex. *J. Atmos. Sci.*, **38**, 1664–1674.

Newell, R. E., and S. Gould-Stewart, 1981: A stratospheric fountain? *J. Atmos. Sci.*, **38**, 2789–2796.

Ninomiya, K., 1971: Dynamical analysis of outflow from tornado-producing thunderstorms as revealed by ATS III pictures. *J. Appl. Meteor.*, **10**, 275–294.

——, M. Ikawa and T. Akiyama, 1981: Long-lived medium scale cumulonimbus cluster in Asian subtropical humid region. *J. Meteor. Soc. Japan,* **59,** 564–577.

Nitta, T., 1977: Response of cumulus updraft and downdraft to GATE A/B-scale motion systems. *J. Atmos. Sci.,* **34,** 1163–1186.

O'Brien, J. J., 1970: Alternative solutions to the classical vertical velocity problem. *J. Appl. Meteor.,* **9,** 197–203.

Ogura, Y., and M.-T. Liou, 1980: The structure of a midlatitude squall line: A case study. *J. Atmos. Sci.,* **37,** 553–567.

Rutledge, S. A., and D. R. MacGorman, 1988: Cloud-to-ground lightning in the 10–11 June 1985 mesoscale convective system observed during O.K. PRE-STORM. *Mon. Wea. Rev.,* **116,** 1393–1408.

——, R. A. Houze, Jr., M. I. Biggerstaff and T. Matejka, 1988: The Oklahoma–Kansas mesoscale convective system of 10–11 June 1985: Precipitation structure and single-Doppler radar analysis. *Mon. Wea. Rev.,* **116,** 1409–1430.

Schlesinger, R. E., 1984: Mature thunderstorm cloud-top structure and dynamics: A three-dimensional numerical simulation study. *J. Atmos. Sci.,* **41,** 1551–1570.

Simpson, J., R. F. Adler and G. R. North, 1988: A proposed tropical rainfall measuring mission (TRMM) satellite. *Bull. Amer. Meteor. Soc.,* **69,** 278–295.

Webster, P. J., and G. L. Stephens, 1980: Tropical upper-tropospheric extended clouds: Inferences from Winter MONEX. *J. Atmos. Sci.,* **37,** 1521–1541.

Yanai, M., S. Esbensen and J. H. Chu, 1973: Determination of bulk properties of tropical cloud clusters from large-scale heat and moisture budgets. *J. Atmos. Sci.,* **30,** 611–627.

Zhang, D.-L., K. Gao and D. B. Parsons, 1989: Numerical simulation of an intense squall line during 10–11 June 1985 PRE-STORM. Part I: Model verification. *Mon. Wea. Rev.,* **117,** 960–994.

——, and ——, 1989: Numerical simulation of intense squall line during 10–11 June 1985 PRE-STORM. Part II: Rear inflow, surface pressure perturbations and stratiform precipitation. *Mon. Wea. Rev.,* **117,** 2067–2094.

Zipser, E. J., 1977: Mesoscale and convective-scale downdrafts as distinct components of squall-line circulation. *Mon. Wea. Rev.,* **105,** 1568–1589.

——, 1988: The evolution of mesoscale convective systems: Evidence from radar and satellite observations. *Tropical Rainfall Measurements.* J. S. Theon and N. Fugono, Eds., A. Deepak, 159–166.